Review Article

Tribological Behavior of Functionally Graded Composite Materials

A. Rabieifar[1,2], H. Sabet[3,4*], A. Asaadi Zahraei[5]

[1]Department of Materials Engineering, ST.C., Islamic Azad University, Tehran, Iran.
[2]Advanced Materials Engineering Research Centre, Ka.C., Islamic Azad University, Karaj, Iran.
[3]Department of Materials Engineering, Ka.C., Islamic Azad University, Karaj, Iran.
[4]Institute of Manufacturing Engineering and Industrial Technologies, Ka.C., Islamic Azad University, Karaj, Iran.
[5]Faculty of Materials Science and Engineering, Khajeh Nasir Toosi University, Tehran, Iran.
Received: 03 December 2024 - Accepted: 28 *May 2025*

Abstract

The Tribological performance of Functionally Graded Composite Materials (FGCM) under abrasive and reciprocating test conditions is reviewed from the numerous studies performed over the last three decades. FGCM produced differing wear analysis trends under varying process conditions and parameters. A general framework identifying the process parameters and assessing the wear performance through wear modes and mechanisms is presented. The tribe system material loss is reduced by optimizing the process parameters independently for specific engineering applications depending on the industrial demands. Moreover, the different challenges faced during wear analysis were discussed, and their prospects in various scientific and technological fields were addressed.

Keywords: Tribological Behavior, Abrasive Wear, FGCM, Wear Mechanism.

1. Introduction

Industrial applications involving friction and wear, such as pump parts, cylinders, bearings, and moving parts, require specific material properties, which limits the range of materials (metals, alloys, and conventional composites) chosen for fabrication.[1]

This led to the development of functionally graded materials (FGM), an evolutionary material that displayed gradient material properties and provided superior location-specific performance [2]. These materials have shown potential in a wide range of aerospace, automobile, defense, and other industrial applications that require high surface wear resistance as well as interior bulk material toughness at relatively high temperatures, which was not achievable in monolithic metal matrix composites (MMC) [3, 4]. FGMs manufactured by designers are usually categorized based on component mixtures such as ceramic/metal, ceramic/ ceramic, metal/metal, and ceramic/polymer, where ceramic/metal is the most widely used combination of materials [5, 6]. Due to their ability to take advantage of improved mechanical properties such as stiffness, resilience, machinability, and durability, as well as increased thermal, wear, and corrosion resistance, ceramic/ metal FGMs have gained widespread attention [7, 8]. FGC fabrication processes, including solid, liquid, and gas-based methods, range from vapor deposition to spraying methods [9, 10]. Each processing method had a defined set of parameters that influenced the final properties of the FGM. Hence, the choice of fabrication method depends mainly on the desired material properties, industrial application, material composition, component geometry, and the suitability and feasibility of production methods [11]. Wear involves gradual material removal of a surface that is in relative motion with another surface through mechanical and/or chemical processes. Wear is observed in various industrial applications such as automobile brakes, gears, bearings (plain and ball), agricultural equipment, earthmovers, and slurry pumps, and daily life applications such as knives, tools, and furniture, and also in human beings in the form of bone wear at joints of hip, elbow, and knee [12]. Under continuously varying process parameters, a surface is subjected to multiple wear mechanisms. Underwear processes are classified based on wear mechanisms such as adhesive, abrasive, fatigue, and tribo-chemical wear, depending on the system's kinematics. Researchers further define variations of the abovementioned classifications as impact, erosive, corrosive, cavitation, oscillation, and softening. Fig. 1. represents the different wear modes and wear mechanisms experienced by FGCs. Abrasive wear occurs due to the movement of hard asperities between the two surfaces in motion against each other. This damages the interface of the softer surface through plastic deformation or fracture. Adhesive wear is developed due to the formation and detachment of adhesive bonds at the interface of two surfaces in sliding contact, whether they are lubricated. For this mechanism, wear develops with subsequent adhesions and peeling in the remaining area of surfaces in contact [13, 14].

*Corresponding author
Email address: hamed.sabet@iau.ac.ir

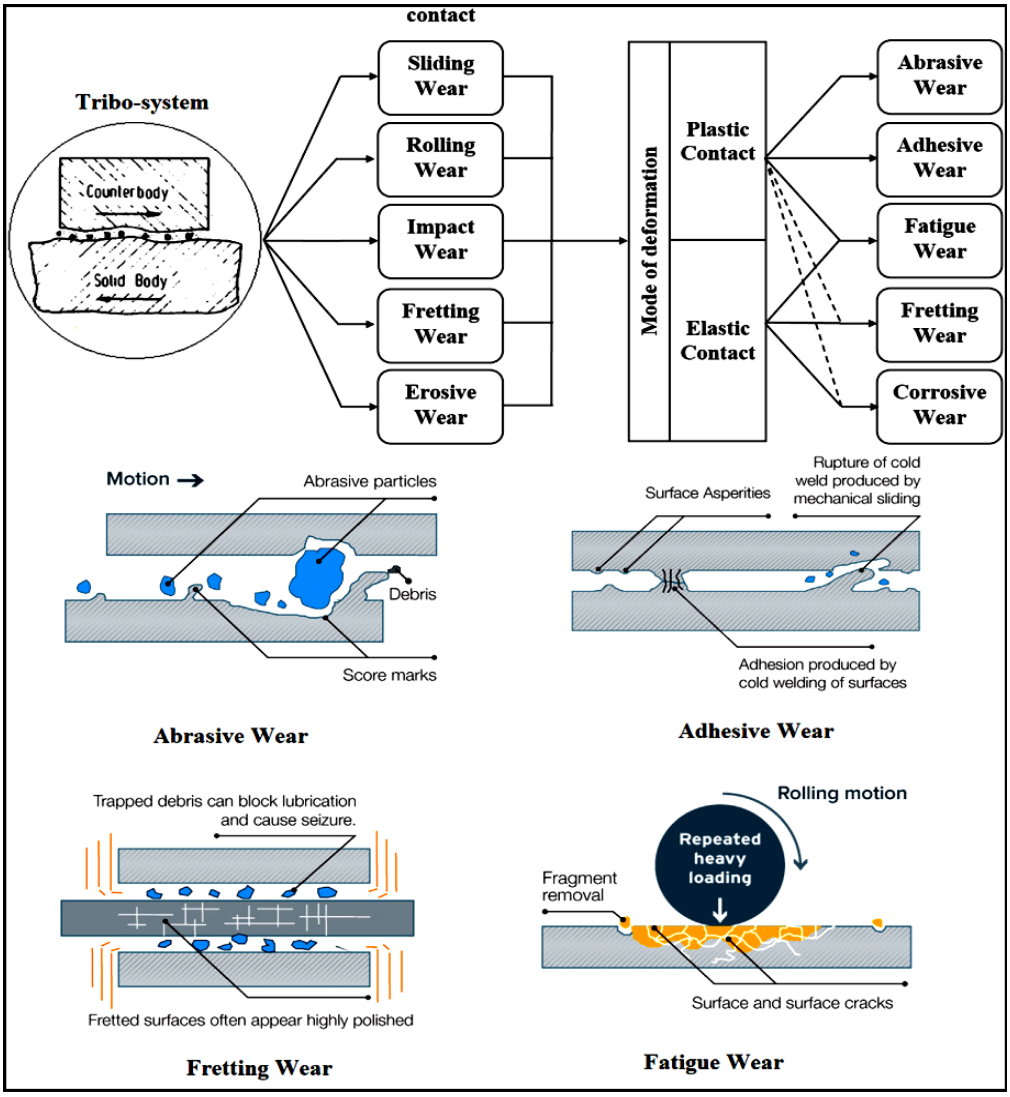

Fig. 1. Classification and illustration of wear modes and wear mechanisms [13].

The wear performance of FGCs is influenced by various tribological parameters, classified into mechanical and physical factors (extrinsic) and material factors (intrinsic).

Extrinsic parameters involve mechanical factors such as load, sliding velocity, and sliding distance and physical factors such as reinforcement particle orientation, ambient conditions, the surface finish of the sample, and counterface. Intrinsic factors involve material parameters such as reinforcement shape, type, size, volume fraction, and particle distribution [15]. FGMs have evolved to include metallic, ceramic, and polymer composites for various industrial tribology applications, such as engine cylinders and pistons, which undergo abrasive and reciprocal sliding; it is critical to investigate the behavior of FGCs under varying intrinsic and extrinsic parameters [16]. This review article defines the current status of research and development conducted on FGCs under abrasive and reciprocating test conditions. The influence of intrinsic and extrinsic parameters on the wear behavior of the FGCs processed through different manufacturing routes is also explored, highlighting the importance of process parameters on the wear behavior.

2. Abrasive Wear Test in FGCs

Abrasive wear exists as two- or three-body wear (Fig. 2.) [17]. Two-body abrasion occurs due to hard protruding particles on the counterface, or asperities on the surface (rough and hard) in contact with a second surface, chipping the softer surface. Three-body abrasion occurs when these particles are pulled out and are free to roll and slide between the sliding surfaces [12]. Depending on the motion of the free particles, researchers define two and three-body abrasive wear as sliding abrasion and rolling abrasion. Abrasive wear exists in three different modes, such as micro-cutting, wedge forming, and ploughing (Fig. 3.) [13]. During a process, the wear occurs in one mode, transitions from one mode to another, or acts simultaneously [18]. For the micro-

cutting mode of wear, long curled ribbon-like wear debris was formed, wedge-shaped wear debris was formed for the wedge form of wear, whereas for ploughing, a shallow groove-like feature was formed on the specimen surface [19].

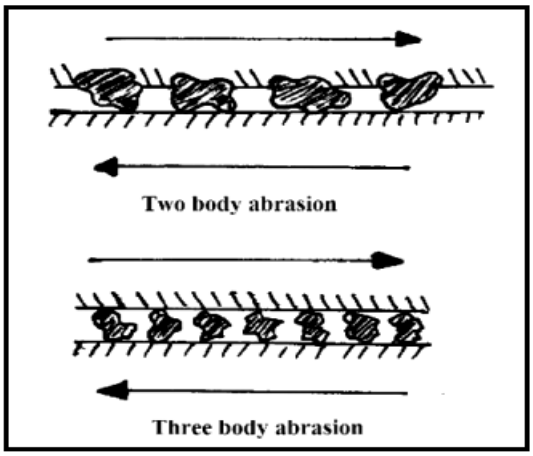

Fig. 2. Illustration of different types of abrasive wear [17].

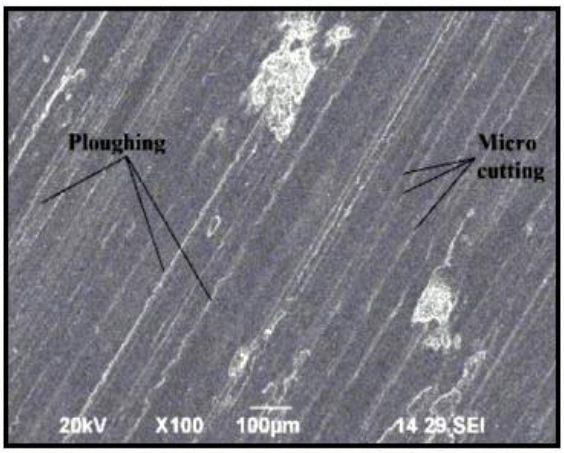

Fig. 3. Different modes of abrasive wear as observed under SEM [13].

The abrasive wear response of FGCs is experimentally analyzed using laboratory tests such as a specimen sliding against a fixed abrasive sheet or a rotating wheel or a ball sliding against a plane specimen with loose abrasive particles being continuously fed between the sliding surfaces.

The first three methods involve fixed abrasive particles, which cause two body abrasive wear on the specimen. Abrasive paper or cloth (Silicon carbide or Alumina) with evenly distributed grit particles of narrow size is used as the counterface face [20].

The rubber wheel abrasion test involves loose abrasive particles (Quartz or Silica sand) either as a powder or mixed with a liquid to form a slurry; a specimen in the form of a plate or block was pressed against the rotating rubber wheel under constant load. Specimens subjected to wheel abrasion experienced a combination of rolling and sliding motion wear scars. The specimen pin sliding on a fixed abrasive sheet produced two-body sliding wear features [21]. Fig. 4. shows the illustration of different abrasive wear tests.

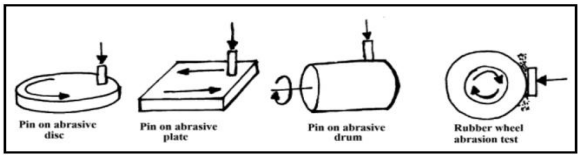

Fig. 4. Illustration of different types of abrasive wear test [21].

2.1. Effect of Abrasive Medium

Abrasive media hardness, size, and shape significantly affected the specimen wear rate through various wear mechanisms. Hard abrasive particles ploughed out the softer phases and created larger ones, whereas soft particles dug out small phases or produced larger ploughing pits. These fractured particles behaved as abrasive particles, increasing the wear [22]. The ratio of abrasive particle hardness (Ha) to surface hardness (Hs) significantly influenced the wear behavior. The wear rate became sensitive when Ha/Hs < ~1, the abrasive particle indented the specimen when Ha > ~1.2Hs, and the particle underwent blunting when Ha < ~1.2Hs [13].

The abrasive wear rate was influenced by the shape of abrasive particles, with sharp and angular-edged abrasive particles generating much higher wear than smooth and rounded particles [23]. Fig. 5. depicts the different abrasive media used for abrasive wear tests.

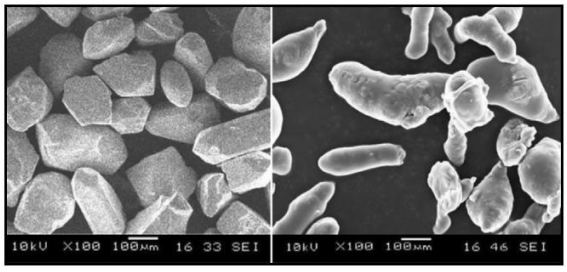

(a) (b)

Fig. 5 SEM micrographs of (a) silica sand (b) alumina particles [24].

Abrasive particles of varying sizes significantly influenced the material removal, with the wear rates significantly low for particles smaller than 100 µm [24]. For abrasive and erosive wear modes, abrasive particle size ranged between 5 and 500 µm, particle size<1 µm was employed for polishing, whereas for gouging wear, particle size ranged between 10 and 100 mm. The extreme edges and sharp corners of

large angular-shaped particles appeared predominantly round-shaped particles and depended mainly on the penetration depth of the specimen [22, 25]. Abrasive grit penetration and particle size influenced the critical variable relative penetration depth, which defined the relative abrasive wear resistance of the composite having constant reinforcement volume fraction [26]. The wear resistance increased significantly if the variable value was less than unity and was independent of the penetration depth when the ratio was greater than unity. The abrasive wear resistance for an FGC depended on the reinforcement particle and abrasive media hardness [27].

2.2. Effect of Matrix Alloy and Secondary Phases

The abrasive wear rate was largely dependent on the rheological behavior of the matrix alloy, the hard secondary phase particles present in the matrix, and their corresponding physical parameters such as size, shape, hardness, volume fraction, and particle orientation. It also depended on the alloy properties and the interfacial bonding between the secondary phase particles and matrix. Molten metals and alloys are Newtonian fluids, with viscosity known to be independent of shear rate [28]. According to the Arrhenius relationship, the viscosity of molten metal decreases with increasing melt temperature. When reinforcement particles are added to the melt, the viscosity rises dramatically, the melt becomes non-Newtonian, and the melting fluidity decreases. As solid particles are dispersed in the liquid melt, particle-melt and particle-particle interactions occur, which increases the slurry's apparent viscosity and aids in the dispersion of secondary phase particles in the melt [28]. Due to their good strength, exceptional wear, and corrosion resistance, aluminum, copper, and its alloys found themselves as highly demanding materials for wear applications. Copper increased the matrix viscosity by creating a positive gradient particle distribution in the composite. In contrast, magnesium reduced the matrix viscosity and improved the secondary particle wettability with the matrix through the negative particle gradient distribution [28, 29]. The addition of silicon and copper decreased the wear loss of aluminum FGCs synthesized through the gradient slurry disintegration and deposition (GSDD) method when compared to pure Al matrix, with Al-Cu composites displaying superior abrasive wear resistance characteristics than Al-Si and pure Al composites [30]. Fig. 6. shows the SEM micrograph of SiC/Al-Mg at low and high SiC ends. The addition of alloying elements (Sn, Ni, and Si) eliminated the limitations of copper alloy, such as low thermal stability and material strength. This improved the alloy properties and made them viable as a matrix material for wear applications [31]. Titanium and its alloys were used in various high-temperature and high-performance applications involving strength, toughness, corrosion, chemical, and wear resistance. Alloying elements influenced the matrix viscosity and affected the reinforcement particle distribution in the composite [32].

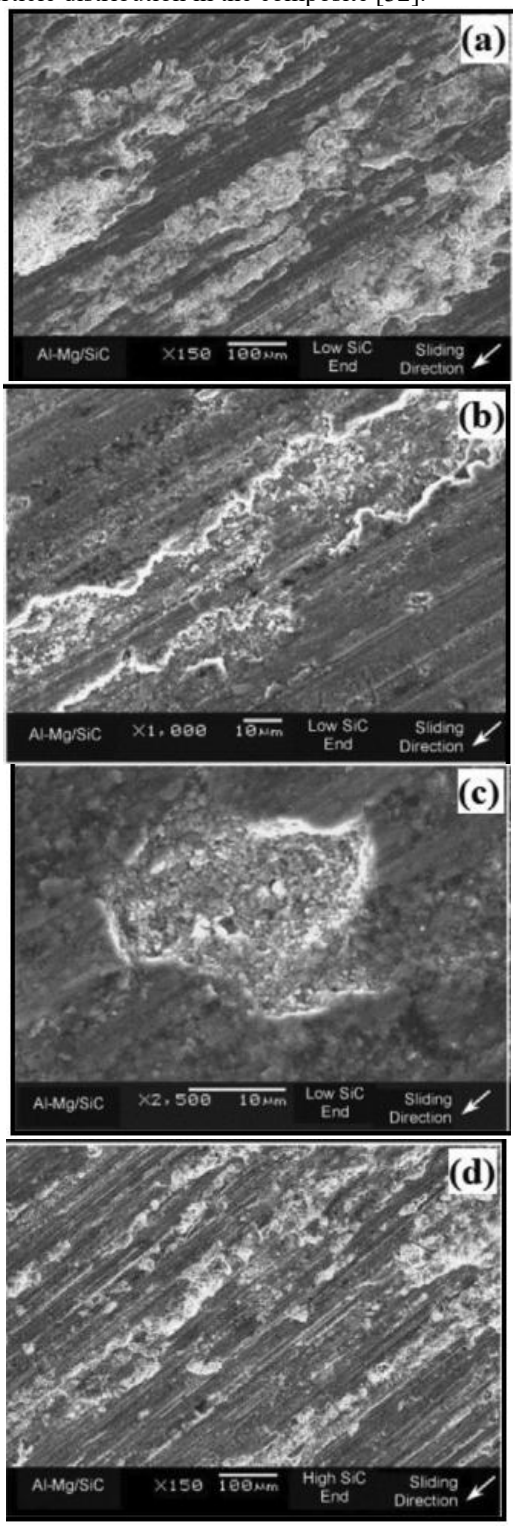

Fig. 6. SiC/Al–Mg SEM micrographs (a) at low SiC end (b) long, shallow craters atlow SiC end caused by delamination (c) particle pull-out at low SiC end caused by delamination (d) at high SiC end [30].

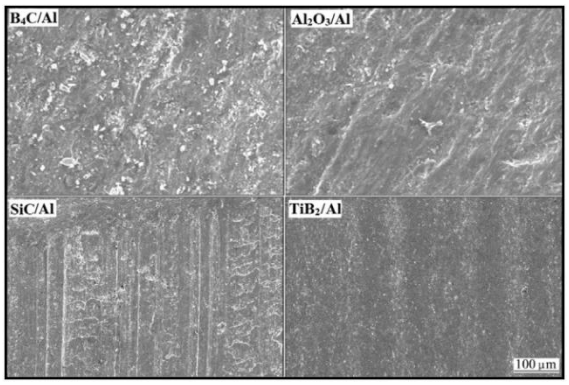

Fig. 7. SEM micrographs of B_4C/Al, Al_2O_3/Al, SiC/Al, TiB_2/Al FGCs [34].

Any matrix alloy limitations were eliminated, and material properties were improved by adding ceramic particles as secondary reinforcement phases. Ceramic reinforcements used in MMCs are usually non-wettable by the metallic melt, necessitating an additional driving force to remove surface energy barriers. Alloy chemistry, particle addition temperature, and stirring intensity are some parameters that govern the wetting of the reinforcement with the melt. In contrast, gravity, buoyancy, or stirring motion are some forces that regulate the motion of particles in the melt. Ceramic reinforcement particles commonly used for improving wear resistance include Boron Carbide (B_4C), Silicon Carbide (SiC), Aluminum Oxide (Al_2O_3), etc. [33].

Abrasive wear resistance was significantly higher for centrifugally cast aluminum FGCs than homogeneous alloy due to the load-bearing secondary phase particles' hardness relative to the matrix hardness [34, 35]. Fig. 7 depicts the SEM micrograph of various reinforcement particles on the abrasive wear behavior of Al-12Si-Cu FGC. The addition of $Al_2O_3$and graphite displayed contrasting results for centrifugally cast copper-based FGCs, with Al_2O_3-reinforced FGC displaying a higher wear rate than graphite-reinforced FGC. This was mainly due to the solid lubrication effect of the added graphite particles, which created a graphite-rich tribo-film for smooth sliding of the specimen over the counterface [36]. The secondary phase characteristics, such as particle shape and size, influenced the wear volume loss, with coarse-sized particles effectively resisting the surface cutting and penetration [37]. The strongly bonded, larger secondary phase particles underwent fracture, blunt, or resist soft abrasive particles, whereas weakly bonded particles were easily pulled off through the abrasive action [38].

Gravitational effects are minimal for particles<10 μm in size and are entirely suspended in the liquid, whereas gravitational forces significantly influence the formation of a particle concentration gradient for particles in the 10–100 μm size range. Particles between 100 and 1000 μm in size are completely suspended at high velocities and often sink and settle to the bottom of the vortex, creating a cluster [37]. The best wear results were achieved for FGCs when secondary phase particle size ranged between 20 and 50 μm [35, 39].

2.3. Effect of Particle Weight/Volume Fraction

The secondary phase particle weight/volume fraction significantly influences the graded layer particle concentration, subsequently affecting the abrasive wear response.

A sharp decrease in wear volume loss was observed as the reinforcement content increased up to 5% in centrifugally cast FGCs, whereas a much slower decrease in wear volume was observed as volume fraction increased above 5% [40]. During fretting and sliding, up to ~ 20% improvement in the abrasive wear performance was observed with an increase in the ceramic particles' weight/volume fraction. Above the critical volume fraction, the second-phase particles were either pulled out or underwent partial fracture, increasing the three-body abrasion rate [41]. The abrasive wear performance of centrifugally cast composites with reinforcement weight fractions varying between 5 and 20 wt% was analyzed, and 10 wt% was considered as the optimum concentration to obtain a homogenous distribution of particles. This helped avoid reinforcement particle cluster formations, thus enhancing the wear characteristics [42]. Fig. 8 shows the wear micrograph of as-cast Al-6.5% SiC FGC and the surface features observed under SEM. Features (1) denote matrix cracks, (2) represent fine grooves (abrasion), (3) denote the oxide formations, and (4) represent the particulate pull-out zones (delamination wear) [43].

2.4. Effect of die Rotation Speed and Melt Pouring Temperature

The die rotation speed, melt pouring temperature, die temperature, stirring speed, and stirring time are all process variables that influence the gradient distribution of particles in centrifugally cast composites and simultaneously influence properties such as hardness and wear resistance.

However, according to the literature analysis, the main parameters that influence the performance are die rotational speed and pouring temperature, so the effect of these parameters on abrasive wear rate is summarized. The abrasive wear rate depends on the gradient particle distribution, influenced by die rotation speed and particle density. Increasing rotational speed leads to the advancement in refinement, reinforcement particle segregation, and liquid mass volatility at low speeds. This affected the hardness and, simultaneously, the wear resistance [44].

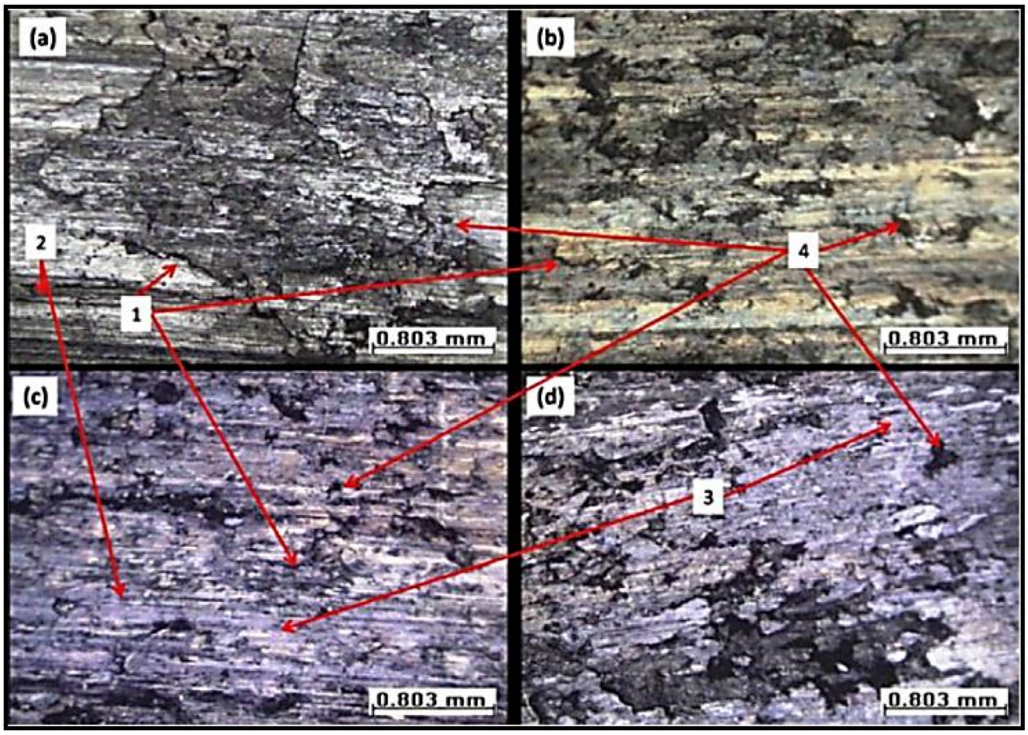

Fig. 8. AA7075-6.5%SiC FGC wear micrographs at (a) 15 N and 2 m/s (b) 15 N and 5 m/s (c) 30 N and 2 m/s and (d) 30 N and 5 m/s [43].

Studies performed in the field of centrifugal casting of FGMs concentrated on maintaining the rotation speed between 800 and 1300 RPM to attain uniform particle dispersion and improvement in mechanical properties [45].The higher the speed, the higher the concentration of secondary phase particles on the peripheral layers, and this is associated with the range of 1000 to 1300 RPM, with the exception that there is a sharp gradient of distribution when utilizing high speeds [40]. Melt pouring temperature in the development of FGCs influenced the mechanical properties significantly through the particle distribution in the matrix. With varying melt pouring temperatures, a sharp gradient of particle distribution resulted in variation in mechanical properties, with weak mechanical properties observed at very high pouring temperatures.

Most studies focused on a pouring temperature range of 700–850 ˚C, with the best performance obtained at a melt pouring temperature range of 700–750 ˚C [46]. Gradient distribution of particles with rapid cooling of the solid melt leads to high particle concentration layers, which improve the mechanical properties and, simultaneously, the wear resistance [47]. However, the nature of the transition from particle enriched to depleted zone was dependent on the matrix alloy's freezing range.

2.5. Effect of Wear Process Parameters and Corresponding Wear Mechanism

Countless investigative studies in the relevant field of composites explored the abrasive wear response variations as a function of varying process parameters. Applied load, sliding speed, sliding distance, sliding time, thermal conditions, reinforcement type, etc., were considered the most influential wear process parameters for abrasive wear analysis.

2.5.1. Effect of Applied Load

Abrasive wear analysis of centrifugally cast Al and Cu FGCs under varying applied load conditions revealed linearly increasing wear rates and three specific wear regimes with increasing process conditions. Centrifugally cast Al-Si composites at low load displayed mild wear, characterized by fine scratches and shallow grooves. Mild wear had transitioned into combined plowing and cutting wear regimes at intermediate loads, characterized by predominant wear grooves developed due to continuous abrasive particle action [34, 48, 49]. A critical load exists beyond plastic deformation, characterized by severe cutting and micro-plowing due to dislodged reinforcement particles [50]. Continuous abrasive particle action caused a transition in the wear mechanism from plowing wear to erosive wear at extreme load conditions, which is completely unreasonable for aluminum FGCs [34, 39]. A combination of plowing and erosive wear defined the wear response of Si_3N_4/Al FGC at 80 N applied load, with the graded composite displaying superior wear resistance over the homogenous composites at low loads [39]. Abrasive wear characterized by longitudinal grooves

and scratches defined the wear behavior at low load (10 N) for SiC/Cu-10Sn FGC synthesized through horizontal centrifugal casting, which transitioned into combined adhesion and delamination wear at high load (30 N) [51]. Wear performance analysis of SiC/A319 (10, 20 wt%) FGCs at varying applied loads (10–40 N) revealed a transition in wear mechanism from abrasive wear to a combination of abrasion and adhesion mode of wear with predominant abrasion grooves, craters, and delamination wear [52]. Sliding wear behavior study of pulse electrodeposited Ni-Fe-Co and Ni Fe-Al_2O_3 coatings on carbon steel substrates against pin-on-disc setup at varying applied load conditions, revealed mild abrasive wear at low load conditions, which transitioned into a combination of micro cutting, delamination, and plastic deformation with increasing load (Fig. 9.) [53].

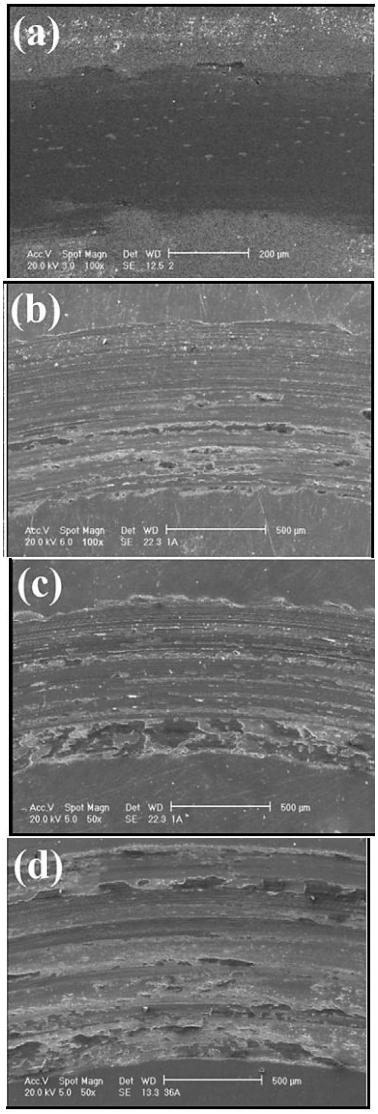

Fig. 9. Wear morphologies of Ni-Fe-Al_2O_3 at varying loads (a) 2.5 N, (b) 5 N, (c) 10 N, and (d) 20 N [53].

2.5.2. Effect of Sliding Speed

Abrasive wear studies conducted in the laboratory employ either a pin-on-disc setup with abrasive sheets on the counter plate or a dry wheel abrasion tester wherein abrasive media such as quartz sand is employed.

The sliding speed for the pin-on-disc setup varied between 1 and 20 m/s. In contrast, the wheel rotation speed for the dry wheel abrasion tester varied between 10 and 200 RPM, depending on the industrial application. This variation in sliding and wheel rotation speed produced contrasting abrasive wear responses for FGCs reinforced with ceramic particles, confirming the abrasive wear rate depends on the speed [34, 35].

Abrasive wear analysis of Al_3Ti/Al, TiB_2/Al, TiB_2/Al–4Cu in-situ centrifugally cast FGCs revealed major wear mechanisms such as abrasion and ploughing had influenced the material loss [25, 26]. A negative wear response was observed with increasing wheel rotation speeds for FGCs reinforced with multiple reinforcements (B_4C, Al_2O_3, SiC, TiB_2), with a three-body wear rate dependent on the contact period between the specimen and the rotating wheel.

At 50 RPM, ploughing and erosive wear were observed, which transitioned into abrasive wear at 150 RPM, which further transitioned into minimal abrasion and blunting of reinforcement particles [54]. Similar wear response and mechanisms were observed for Si_3N_4/LM25 FGC, with an outer layer of graded composite exhibiting superior wear resistance than composite and unreinforced alloy [39]. Erosive wear was the dominant wear regime influencing the wear at low wheel rotation speed (100 RPM), which decreased with increasing speed due to reduced contact between the abrasive silica sand particles on the rotating wheel and the specimen [55].

The wear analysis of spray-deposited SiC/Al-20Si-3Cu FGC revealed the wear rate to depend entirely on the particle concentration and other process parameters such as applied load and rotational speed. The abrasive wear regime observed at low load and rotational speeds transformed into oxidative and delamination wear at high load and rotational speeds [56].

Fig. 10. shows the worn surface morphologies of SiC + Gr/Cu FGC observed at 10 and 30 m/s. Features (1) denoted oxide scale formation, (2) represented particle protrusion on the specimen surface, (3) denoted the formed tribo-layer, and (4) represented the groove lines.

The arrow represents the sliding direction, whereas the curved line denotes the wear sheet removed by delamination.

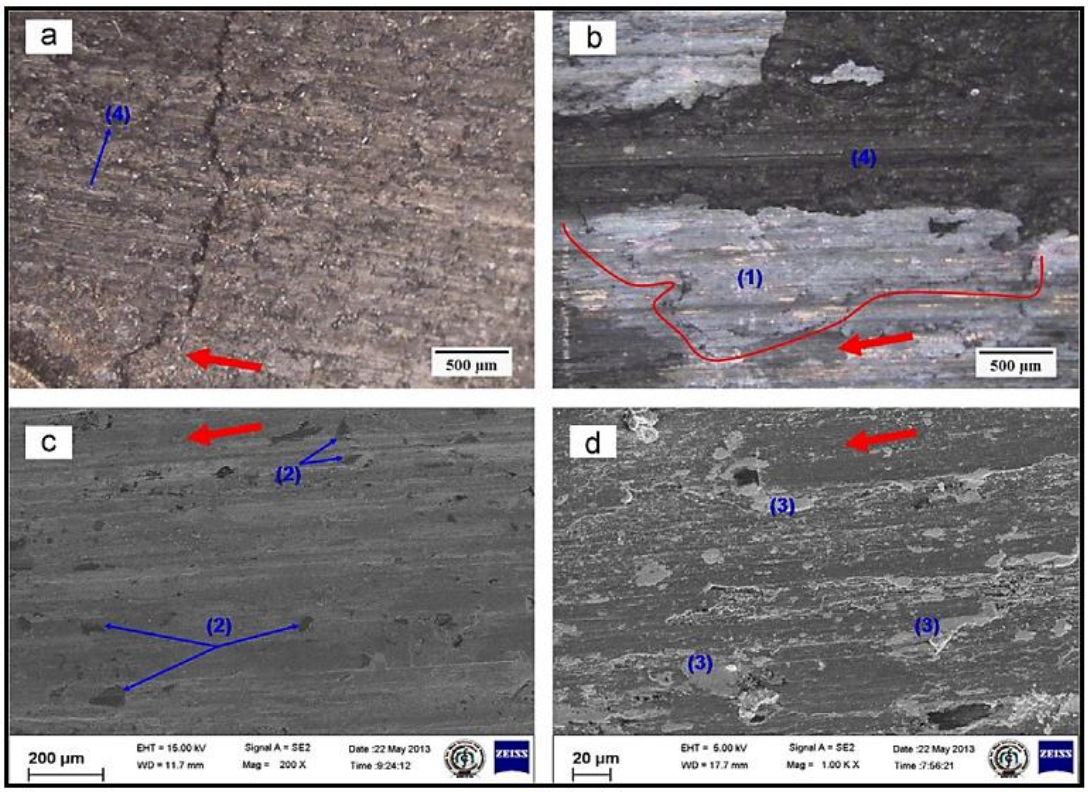

Fig. 10. Worn surface morphologies (a) and (b) macrographs, and (c) & (d) SEM images of SiC + Gr/Cu FGC tested at 10 m/s and 30 m/s respectively [57].

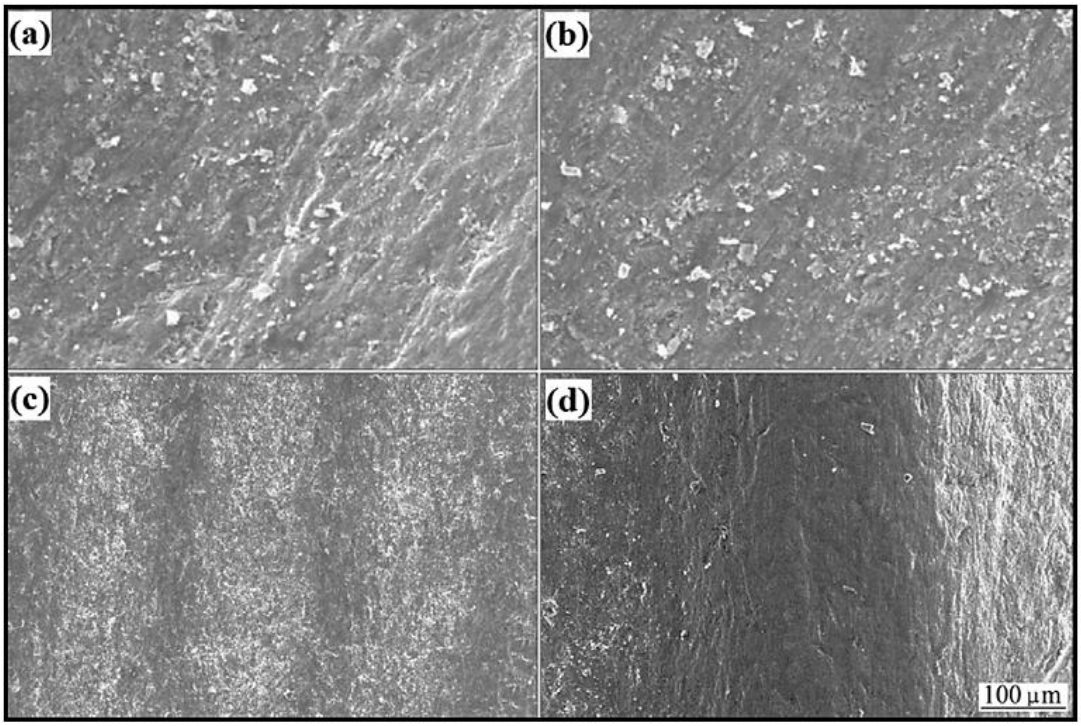

Fig. 11. Wear micrographs Al2O3/Al-12Si-Cu FGC at (a) 3 (b) 5 (c) 7 (d) 9 min [29].

2.5.3. Effect of Sliding Time

The abrasive wear behavior of centrifugally cast Al_2O_3/Al-5Si-3Cu FGC was defined through two specific wear regimes with increasing sliding time. Wear was characterized by initial cutting and abrasive action at shorter durations due to both abrasive media and secondary phase particles. At longer durations, the specimen surface underwent smoothening due to blunting of secondary particles [58].

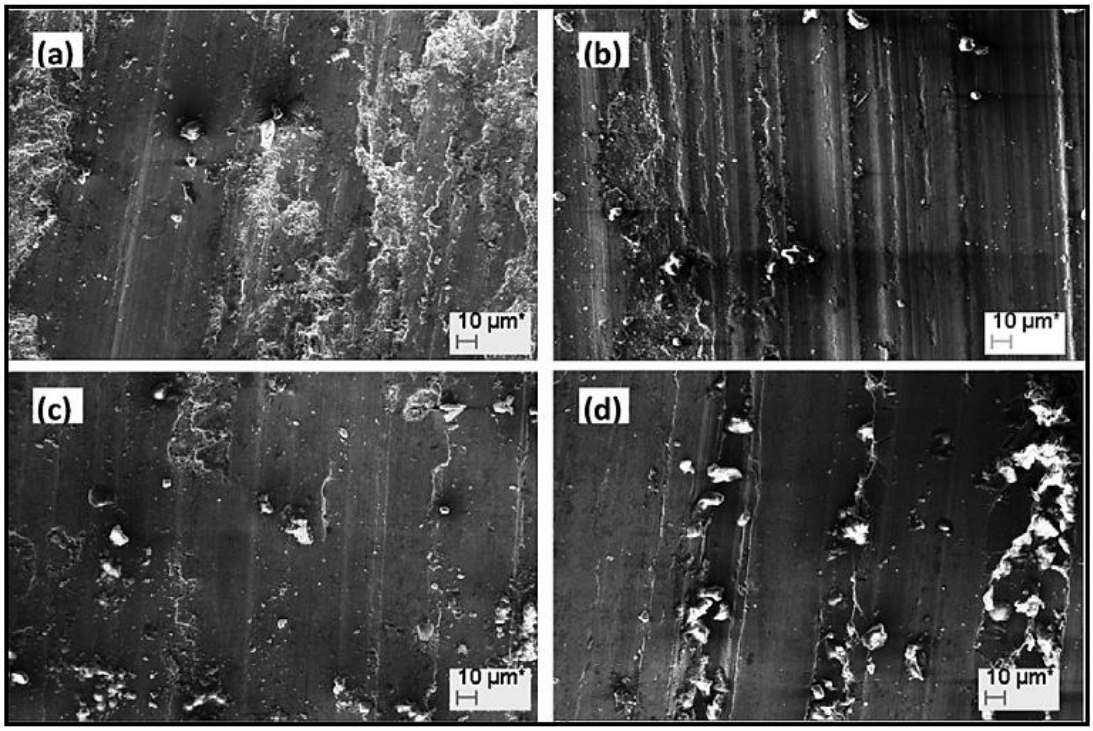

Fig. 12. SEM micrographs of A390-0.5 Mg FGC worn out surface at different loadconditions (a) at 1 kg (piston head(b) at 4 kg (piston head) (c) at 1 kg (skirt region) (d) at 4 kg (skirt region) [54].

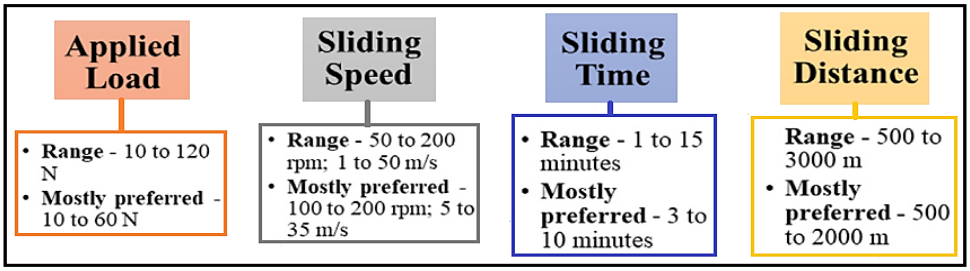

Fig. 13. Experimental ranges for wear process parameters and their optimum values.

Table 1. Summary on the abrasive wear studies of various FGCs and corresponding wear mechanisms.

FGC System		Wear Process Parameters					Mechanisms Observed	Ref. No.
Alloy	Reinforcement	Load (N)	Rotation Speed (RPM)	Sliding Speed (m/s)	Sliding Time (min)	Sliding Distance (m)		
Al-5Si-3Cu	SiC	33-80	100-200	-	5	-	Abrasion, Cutting, Ploughing	[45]
AlSi12Cu	ZrO_2	33-80	100-200	-	5	-	Abrasion, Erosion	[64]
A356	SiC	10-120	-	1	-	330	Abrasion, Adhesion	[47]
LM13	TiB_2	33-57	75-125	-	10	-	Abrasion, Ploughing	[49]
Al-5Si-3Cu	B_4C	28-52	200	-	5	-	Abrasion	[65]
Ti_6Al_4V	WC	25	-	0.02	-	2000	Abrasion, Adhesion	[66]
Al	TiB_2	1, 2	-	3.5	-	75	Abrasion, Erosion	[67]
A413	Al_3Ni	10	530	-	10	-	Abrasion, Delamination	[68]
Al	$TiAl_3$	2	100	-	-	1000	Abrasion, Delamination	[69]
Al-Si	Gr	10-30	-	1.5	-	1800	Abrasion, Delamination	[70]
Al-Ni	SiC	103, 154	-	0.3, 0.9	-	2000	Abrasion, Adhesion	[71]
Ti6Al4V	TiC	20	100	-	15	-	Abrasion, Adhesion	[72]

Al-12Si-Cu FGCs reinforced with multiple reinforcements (B_4C, Al_2O_3, SiC, TiB_2) revealed a similar wear behavior with increasing sliding duration. Abrasive, cutting, and erosive mechanisms defined the wear at smaller sliding durations, whereas blunting of reinforcement particles and smoothening of the specimen surface occurred for longer sliding durations, reducing material loss (Fig. 11.) [34]. Abrasive wear characterized by the cutting and minor particle pull-outs was initially observed for smaller sliding durations, whereas a severe plowing wear regime characterized by increased reinforcement particle pull-outs and material removal was observed for the higher sliding duration [42].

2.5.4. Effect of Sliding Distance

Centrifugally cast WC/LM25 FGC reported a non-linear wear trend followed by a linear trend with increasing sliding distance at constant applied load [59]. This behavior was characterized by a transition in wear mechanism from mild abrasion to severe adhesion wear to mild lubrication wear [59]. Al-12Si-Cu FGCs reinforced with B4C, SiC and ZrO_2 reinforcement particles displayed contrasting results, wherein a linear relationship was observed with increasing sliding distance [59]. For dry sliding analysis performed on FGCs, abrasion wear was reported as the dominant wear regime influencing the specimen pin and hardened steel counterpart at a low sliding distance. This later transformed into abrasion wear for the counter face and adhesion-induced tribo fracture for the specimen pin during steady-state sliding [51, 60].

2.5.5. Effect of thermal and lubrication conditions

Thermal treatment enhanced the abrasive wear response of the composite through grain refinement and precipitation hardening, which improved the micro-hardness and wear resistance. The addition of 0.5% Mg increased the rate of Mg precipitation (in alloy). It formed hard in-situ primary silicon particles, which improved the hardness and wear resistance of centrifugally cast A390-0.5% Mg piston head, interface, and skirt regions [54]. The SEM micrographs of A390-0.5 Mg FGC worn out surface at different load conditions and the experimental ranges for wear process parameters and their optimum values are shown in Figs. 12 and 13, respectively. The Summary on the abrasive wear studies of various FGCs and corresponding wear mechanisms are mentioned in Table 1.

3. Reciprocating Wear in FGCs

Low hardness and poor tribological performance of aluminum alloy components greatly restrict their range of applications within the automotive industry. The rate of wear due to interfacial friction iscontrolled by improving the alloy hardness through ceramic coating or by addition of ceramic particles as reinforcement [73]. For aluminum composites, the dominant wear mechanisms observedwere two-body abrasive wear, adhesive wear, oxidative wear, and delamination. Reduction in friction coefficient was better regulated through tribo-film formation [74]. Fig. 14. shows the illustration ofdifferent types of linear reciprocating wear tests.

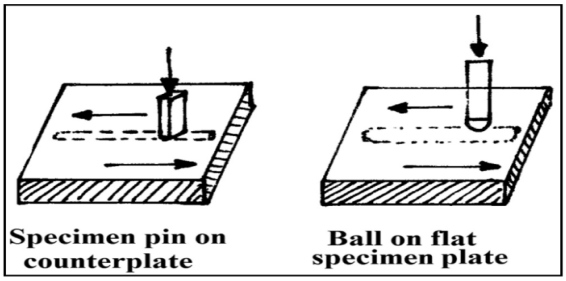

Fig. 14. Different types of reciprocating wear tests.

3.1. Effect of Composition

The third body formation rate directly depended on the concentration and type of ceramic particles, lubrication at the sliding interface, and load conditions. This mode of material removal by the third body particles largely impacted the steady state of the reciprocating systems through severe surficial scratching. It was followed by an initiation of tribo-layer phenomena [75]. Hybrid ceramic coating of oxy-trio ceramics-60 vol% Al_2O_3, 20 vol% ZrO_2, and 20 vol% TiO_2 on Al6061 substrate improved the wear and heat resistance and the tribology performance [76]. Under dry sliding reciprocating conditions, the frictional coefficient of aluminum substrates coated with ceramic compounds was observed to be greater than or equal to that of cast iron when tested against a chrome-plated counter-face material [77]. Fig. 15. shows the subsurface structure (a-b) of coarse-grained Cu-0.3Al alloy and its corresponding EBSD analysis (c-d) when subjected to reciprocating wear. EBSD map shows dynamic recrystallization grains (blue), subgrains (yellow), and deformed grains (red). Reciprocating wear analysis of 15%SiC/A319, 15%SiC/A336, and 15%SiC/A390 composites under varying wear process parameters revealed predominant adhesive wear behavior assisted by severe plastic deformation and material removal. SiC/A390 composite displayed better stability and could withstand severe wear under extreme testing conditions up to a transition point towards higher load/velocity owing to the higher silicon content [79]. Intensive adhesive wear and severe deformations characterized by small patches, shallow grooves, and small dimples defined the wear behavior of Ti/TiN/Si multilayer-coated Al FGC composite under combined compressive and shear stresses along the sliding direction [80].

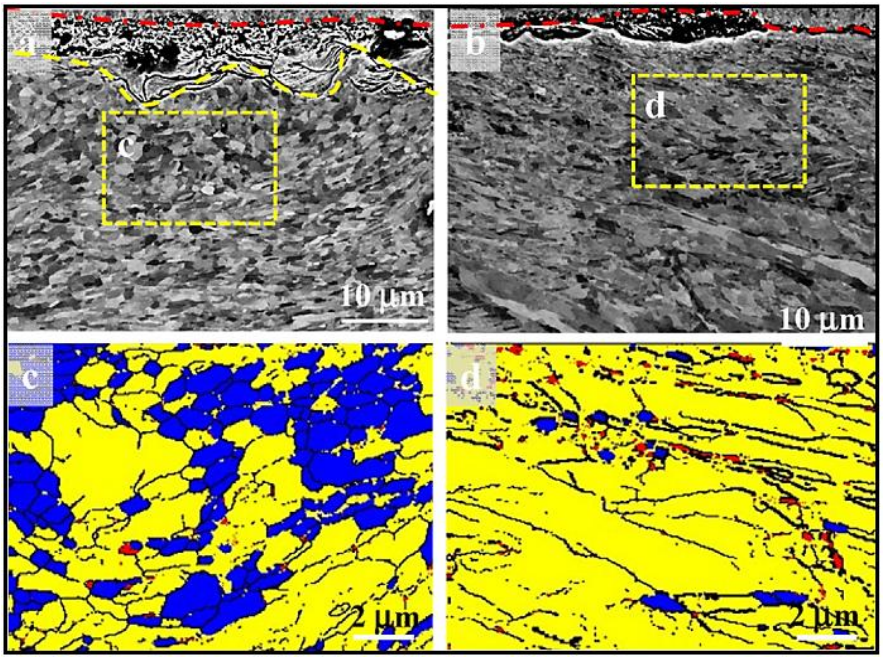

Fig. 15. Cross-sectional view of reciprocating tribo-subsurface structure of (a, b)coarse grained Cu-0.3Al alloy and its corresponding EBSD analysis (c, d) [78].

3.2. The Effect of Process Parameters and Corresponding Wear Mechanisms

Wear mechanismsduring the reciprocating wear behavior of graded composites was studied by varying applied load, sliding distance, and reciprocating velocity.

3.2.1. Effect of Applied Load

Tribology analysis performed at varying normal loads confirmed that a rise in applied load substantially influenced the wear mechanisms through enhanced surface deterioration under in situ sliding conditions. At low load (<20 N), the composites experienced a tendency to undergo minor delamination initiations along with removing the thin surficial layer. As the applied load increased, a gradual transition to parallel and shallow channel grooves was reported, along with pits and deeper delamination along the sliding direction. Further load rise to a higher magnitude (>50 N) reported reduced pits and groove formation. In addition, delaminated sheets and crevice formations were prevalent (Fig. 16.) [81]. The adhesive wear regime defined the wear behavior of 10SiC/A356 FGC at low loads (<10 N); in contrast, the wear mode transformed into a combination of adhesive and abrasive wear regimes with increasing applied load. Due to the higher concentration of ceramic reinforcement particles along the sliding surface, a transition from adhesive to oxidative wear regime was observed, leading to a decline in the wear rate. At higher loads (>10 N), large pit formations were observed due to a higher rate of SiC particle pullouts [82].

Tribo-mechanical behavior of as-cast and heat-treated A359/6wt.%Ti-based (TiB_2, TiO_2, and TiC) composites was investigated under varying normal loads (15–55 N). Analysis revealed wear rate to be directly dependent on applied load. Wear analysis revealed severe delamination wear at an intermediate load (35 N) due to excessive ceramic pull-out caused by third-body abrasive wear [83]. Wear micrograph of 15%SiC/A319 composite displayed mild wear behavior with the oxidized surface at 30 N load, transforming into moderate wear with primarily wear scars, crater, and delamination at 60 N. At 90 N load and 1 m/s reciprocating velocity, the worn surface displayed severe wear characteristics with deep grooves and plastically deformed ridges [79] (Fig. 16).

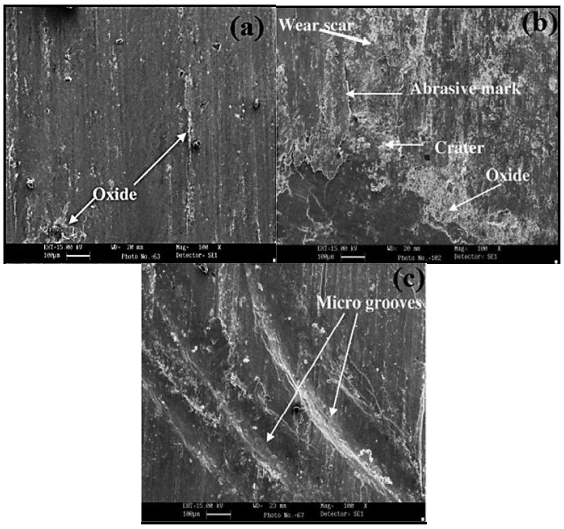

Fig. 16. Wear micrographs of 15%SiC/A319 at (a) 30 N (b) 60 N load and (c) 90 N [79].

3.2.2. Effect of Sliding Distance

Sliding distance is the crucial process parameter that influences the reciprocal sliding wear behavior of FGCs next to the applied load. An increasing trend for wear rate was observed for A359 alloy, SiC reinforced homogenous, and FGCs under increasing sliding distance. It was characterized by a transitional change in wear mechanism from abrasion mode to the combined effect of adhesion and thermal softening of the specimen. Grooves and minimal delamination formation along the sliding direction defined the specimen wear morphology of heat-treated FGC compared to the fretting wear and severe surface damage worn morphology of homogenous and as-cast composites [81]. Fig. 17. depicts SEM micrograph of untreated, heat-treated, and homogenous B_4C/A359 FGCs under varying sliding distances. Dry wear statistical analysis of SiC/Al-Si composites confirms sliding distance (43.65%) as the most influential parameter affecting the wear rate, followed by applied load (23.63%). Analysis revealed a transition in wear regime from mild abrasive wear to severe adhesive and delamination wear under normal load. During this, asperity to asperity contact time and contact area increased with increasing sliding distance, leading to increased wear debris formation [84].

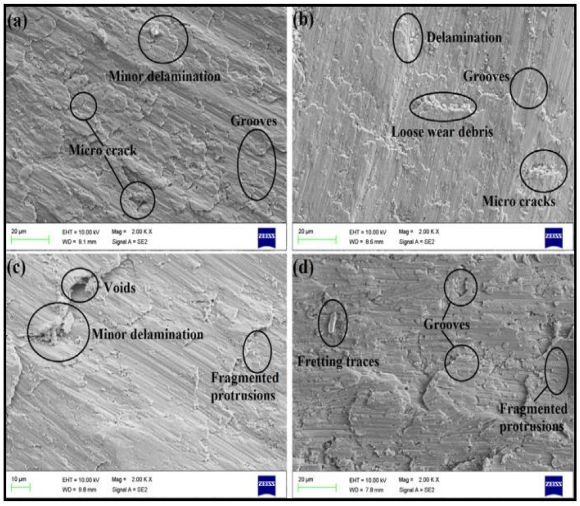

Fig. 17. Worn surface morphology at 1500 mm sliding distance (a) HT FGC (outerzone) (b) HT homogenous (c) as-cast FGC (outer zone) (d) As-cast homogeneous [81].

3.2.3. Effect of Frequency

Friction response during reciprocating sliding for marine cylinder liner materials like cast iron alloyed with chromium, vanadium, and molybdenum revealed a considerable rise at higher contact frequency or a combination of high frequency and small stroke [85].

Meanwhile, a lower frequency (1 Hz) during larger stroke lengths produced low energy per stroke, improving wear resistance [86]. In contrast, during constant frequency (3 Hz) during reciprocating tribology tests, wear response was directly dependent on stroke length, as large strokes increased the duration of sliding action at the same velocity. Higher frequencies (>5 Hz) induced strain hardening effect during dry reciprocating motion and led to a higher wear rate. Vibration induced with higher frequency (>4 Hz) separated contact interfaces while sliding under lower loads. Fig. 18 depicts the SEM image of functionally graded ductile iron pads with smoothened plateaus and areas with torn-off patches when sliding at a frequency of 5.7 Hz [87]. At low load and high frequency, vibration separated the contact interface and lowered the interaction. At higher loads, contact was more prominent to cause severe wear, whereas the wear was controlled in combination with lower frequencies [88].

A reciprocating wear study was performed on SiCp/Al at a constant low frequency of 1 Hz and within a parametric range of 4 mm stroke lengths, 11.4 mm/s sliding velocity, and 4 N normal applied load (at ~ 22 ˚C and relative humidity-40%) exhibiting the least wear volume of 0.00187 mm3 at an optimum reinforcement concentration of 15 wt% [89]. Excellent ceramic-aluminum interfacial bonding decreased the particle pullouts and, in turn, reduced the wear rate. In addition, monitoring of COF was performed as a function of cumulative sliding duration during reciprocating frictional tribo-test of grey cast iron cylinder liner (at a constant stroke length of 2 mm and reciprocating frequency of 10 Hz). It was observed that a periodic drop in mean frictional force occurred with a unit rise in frequency [90]. The data acquisition process exhibited more accuracy with a lower reciprocating frequency (<10 Hz).

Table 2 briefly outlines the various reciprocating wear studies performed on aluminum, copper, and titanium FGCs and their corresponding wear parameter values. The results observed, and the wear mechanisms associated with each study, are also provided.

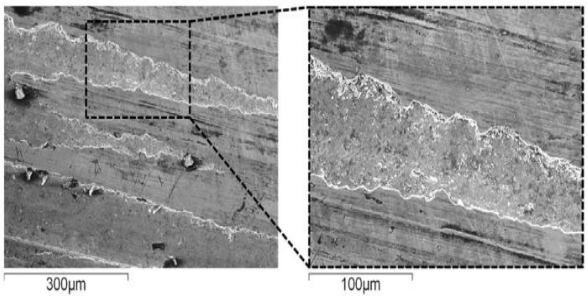

Fig. 18 The SEM image of functionally graded ductile iron pads with smoothened plateaus and areas with torn-off patches at a frequency of 5.7 Hz [87].

Table. 2. Summary on the reciprocating wear studies of various FGCs and corresponding wear results.

FGC System		Wear Process Parameters					Mechanisms Observed	Ref. No.
Alloy	Reinforcement	Load (N)	Frequency (Hz)/No. of Strokes	Reciprocating Velocity (m/s)	Counter Surface Temp. (min)	Sliding Distance (m)		
7075Al, 6061Al	SiC, Al_2O_3	25-75	1605	-	25-110	-	Abrasion, Wear Track	[91]
Duralcan F-3S-20S	SiC	33-80	1, 30 Hz	-	26	-	Fretting, Grooves	[92]
A390	Mg	1-4	-	0.6	-	500	-	[93]
Al-7Si	B_4C	15-35	7 Hz	-	26	500-1500	Tribolayer, Grooves	[94]
Ti6Al4V	TiN/CrAlN	4-13.5	5 Hz	-	25	10-1000	Abrasion, Scars	[95]
Cu-Sn	WC/Co	50	360	10^{-3}	25	400	-	[96]

4. Wear Debris

Wear debris analysis provides insight into industrial machinery's status and helps monitor the specific tribo-system under study. Analyzing the wear debris provides crucial information about the wear mechanism and its formation [97]. The wear debris generated during mild wear was characterized as finely divided particles, and the worn surface was relatively smooth. When wear transitions to severe wear, the generated wear debris is observed to be much larger. Therefore, the wear debris particles were classified as spherical, ribbon, plate, and irregularly shaped based on the wear mechanism or its morphology. Plate-shaped particles are generally flat with a rough perimeter, laminar or wedge-shaped, and have an aspect ratio between 2 and 10. Ribbon-shaped particles are usually curved, long, and skinny, resemble a wire, splinter, or ribbon shape, and have an aspect ratio>10. These particles were formed due to plastic deformation generated by the two-body abrasive action between sharp abrasive particles and the mating surface. Spherical-shaped particles are developed due to the continuous transformation of differently shaped wear particles that could not escape the interface into loose debris with a spherical shape. The particle size is normally<10 μm, and they appear in small numbers and are sometimes fused together. These particles were normally associated with rolling-element bearings and were often a precursor to fatigue failure. Most wear particles generated during adhesive wear and brittle fracture exhibited an irregular morphology, producing irregularly shaped particles [98]. Fig. 19 shows the different wear particle morphology. Analyzing the wear debris morphological characteristics of unreinforced Al alloy (Fig. 20a), the particles were primarily plate-like and ribbon-shaped, a characteristic of a severe wear regime. The wear debris analysis of the R2 region (~4.2% SiC) of FGC cast at 2000 RPM (Fig. 20b) displayed relatively less amount of plate-like and ribbon-shaped wear debris, which was a characteristic of an intermediate wear regime between severe wear and mild wear, whereas the shape and size of loose wear debris particles generated for R3 region (~36% SiCp) of the FGC cast at 1500 RPM characterized a dominant mild wear regime (Fig. 20c) [40].

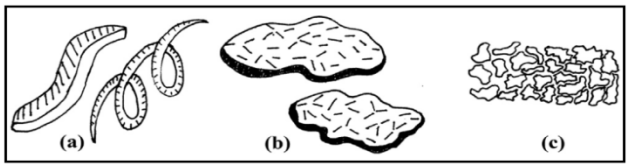

Fig. 19. Wear debris morphology (a) ribbon (b) plate (c) irregular shape [98].

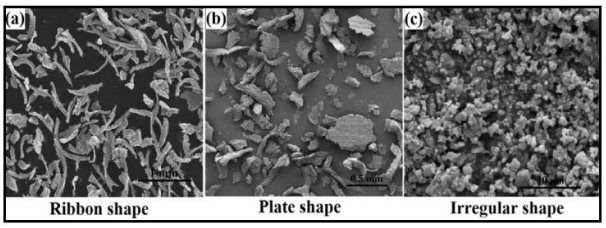

Fig. 20. Wear debris morphology of (a) unreinforced Al alloy (b) FG SiC/Al composite cast at 2000 RPM (c) FG SiC/Al composite cast at 1500 RPM [40].

5. Conclusion

FGCs are rapidly evolving and have become increasingly important due to their superior physical and mechanical properties and their various structural and biomedical applications. This review paper provides an unobstructed and wide view of the sliding wear (abrasive and reciprocating) performance of hard ceramic-reinforced FGCs under varying operative conditions. The abrasive wear performance of FGCs was dependent on the intrinsic (abrasive media, matrix, reinforcement phase, reinforcement particle volume fraction) as well as the extrinsic parameters (applied load, sliding velocity, sliding distance, sliding time, lubrication, and thermal conditions). A detailed insight revealed the intrinsic parameters had a lasting influence on the material's wear resistance, irrespective of extrinsic parameters. Depending on the reinforcement particle shape and size, fabrication

methods, and thermal treatment, the fabricated composite's reinforcement particle gradation and corresponding mechanical properties were significantly enhanced compared to an unreinforced alloy.

Wear in hard ceramic-reinforced FGCs was observed as first body abrasion, oxidation, and adhesion wear in unreinforced alloy and composite metal systems. Third, body abrasive wear was observed in composite–metal systems where the reinforcement particles were not sufficiently tough to bear the load. Unlike rotational wear, reciprocating tribology studies reported a higher percentage of localized wear due to third-body abrasion.

References

[1] Kumar J, Singh D, Kalsi NS, Sharma S, Pruncu CI, Pimenov DY, Rao K, Kapłonek WJ, Comparative study on the mechanical, tribological, morphological and structural properties of vortex casting processed, Al–SiC–Cr hybrid metal matrix composites for high strength wear-resistant applications: Fabrication and characterizations. Mater. Res. Tech. 2020; 9(6):13607–13615.

[2] Katamreddy SC, Punnath N, Radhika N, Multi-response optimization of machining parameters in electrical discharge machining of Al LM25/AlB_2 functionally graded composite using grey relation analysis. Int. J. Mach. Mach. 2018; 20(3):193–213.

[3] Kumar TS, Nampoothiri J, Raghu R, Shalini S, Subramanian R, Development of Wear Mechanism Map for Al–4Mg Alloy/$MgAl_2O_4$ In Situ Composites. Trans. Indian .Inst. Met. 2020; 73:399–405.

[4] Li W, Han B, Research and Application of Functionally Gradient Materials. Mater. Sci. Eng. 2018; 394(2):022065.

[5] Karimzadeh A, Aliofkhazraei M, Rouhaghdam AS, Study on wear and corrosion properties of functionally graded nickel–cobalt–(Al_2O_3) coatings produced by pulse electrodeposition. Bull. Mater. Sci. 2019; 42(53).

[6] Baghal SL, Sohi MH, Amadeh A, A functionally gradient nano-Ni–Co/SiC composite coating on aluminum and its tribological properties. Surf. Coat. Technol. 2012; 206(19-20):4032–4039.

[7] Shanmugasundaram A, Arul S, Sellamuthu R, Investigating the Effect of WC on the Hardness and Wear Behavior of Surface Modified AA 6063. Trans. Indian Inst. Met. 2018; 71:117–125.

[8] Ahmed YM, Sahari KSM, Ishak M, Khidhir BA, Titanium and its alloy. Int. J. Sci. Res. 2014; 3(10):1351–1361.

[9] Boggarapu V, Gujjala R, Ojha S, Acharya S, Chowdary S, Kumar Gara D, State of the art in functionally graded materials. Compos. Struct. 2021; 262:113596.

[10] Naebe M, Shirvanimoghaddam K, Functionally graded materials: A review of fabrication and properties. Appl. Mater. Today 2016; 5:223–245.

[11] Liew KM, Pan Z, Zhang LW, The recent progress of functionally graded CNT reinforced composites and structures. Sci. China. Phys. Mech. Astron. 2020; 63:234601.

[12] Binder M, Klocke F, Doebbeler B, Abrasive wear behavior under metal cutting conditions. Wear. 2017; 376:165–171.

[13] Sevim I. Tribology in Engineering: Effect of Abrasive Particle Size on Abrasive Wear Resistance in Automotive Steels. London: Intech Open; 2013.

[14] Bhushan B, Ko PL, Introduction to tribology. Appl. Mech. Rev. 2003; 56(1): B1–B16.

[15] Basavarajappa S, Chandramohan G, Davim JP, Application of Taguchi techniques to study dry sliding wear behavior of metal matrix composites. Mater. Des. 2007; 28(4):1393–1398.

[16] Saleh B, Jiang J, Fathi R, Al-hababi T, Xu Q, Wang L, Song D, Ma A, 30 Years of functionally graded materials: An overview of manufacturing methods, Applications and Future Challenges. Compos. Part B Eng. 2020; 201:108376.

[17] Kumar GV, Rao CSP, Selvaraj NJ, Mechanical and Tribological Behavior of Particulate Reinforced Aluminum Metal Matrix Composites–a Review. Miner. Mater. Charac. Eng. 2011; 10(1):59–91.

[18] Saleh B, Jiang J, Ma A, Song D, Yang D, Effect of Main Parameters on the Mechanical and Wear Behavior of Functionally Graded Materials by Centrifugal Casting: A Review. Met. Mater. Int. 2019; 25:1395–1409.

[19] Kato K, Micro-mechanisms of wear — wear modes. Wear 1992; 153(1):277–295.

[20] Bhushan B, Modern tribology handbook. 1. Principles of tribology. Bharat: CRC Press; 2001.

[21] Kaushik NC, Rao RN, Effect of applied load and grit size on wear coefficients of Al 6082–SiC–Gr hybrid composites under two body abrasion. Tribol. Int. 2016; 103:298–308.

[22] Manoharan S, Suresha B, Bharath PB, Ramadoss G, Investigations on three-body abrasive wear behaviour of composite brake pad material. Plast. Polym. Technol. 2014; 3:10–18.

[23] Radhika N, Raghu R, Effect of Abrasive Medium on Wear Behavior of Al/AlB_2 Functionally Graded Metal Matrix Composite. Tribol. Online 2016; 11(3):487–493.

[24] Manoharan S, Ramadoss G, Suresha B, Vijay R, Influence of Fiber Reinforcement and Abrasive Particle Size on Three-Body Abrasive Wear of Hybrid Friction Composites. Appl. Mech. Mater. 2015; 766-767:156–161.

[25] Savas Ö, Mater. Application of Taguchi's method to evaluate abrasive wear behavior of functionally graded aluminum-based composite. Today Comm. 2020; 23:100920.

[26] Savas Ö, Investigation of Production and Abrasive Wear Behavior of Functionally Graded

TiB_2/Al and TiB_2/Al–4Cu Composites. Trans. Indian Inst. Met. 2020; 73:543–553.
[27] Radhika N, Raghu R, The mechanical properties and abrasive wear behavior of functionally graded aluminum/AlB_2 composites produced by centrifugal casting Particul, Sci. Tech. 2017; 35(5):575–582.
[28] Hutchings I, Shipway P, Tribology: friction and wear of engineering materials. Cambridge: Butterworth-Heinemann; 2017.
[29] Ahmed A, El-Hadad S, Reda R, Dawood O, Microstructure control in functionally graded Al-Si castings. Int. J. Cast. Met. Res. 2019; 32(2):67–77.
[30] Nai SM, Gupta M, Lim CY, Synthesis and wear characterization of Al based, free standing functionally graded materials: effects of different matrix compositions. Compos. Sci. Tech. 2003; 63(13):1895–1909.
[31] Sasidharan S, Puthucode R, Radhika N, Shivashankar A, Investigation of three body abrasive wear behavior of centrifugally cast Cu-Sn/SiC functionally graded composite using Design of Experiment Approach. Mat. Today 2018; 5(5):12657–12665.
[32] Radhika N, Reghunath R, Sam M. Improvement of mechanical and tribological properties of centrifugally cast functionally graded copper for bearing applications. Proc. Inst. Mech. Eng. C J. Mech. Eng. Sci. 2019; 233(9):3208-3219.
[33] Rajak DK, Pagar DD, Kumar R, Pruncu CIJ, Recent progress of reinforcement materials: a comprehensive overview of composite materials. Mat. Res. Technol. 2019; 8:6354–6374.
[34] Radhika N, Raghu R, Development of functionally graded aluminum composites using centrifugal casting and influence of reinforcements on mechanical and wear properties. Trans. Nonfer. Met. Soc. China 2016; 26(4):905–916.
[35] Radhika N, Raghu R, Abrasive wear behavior of monolithic alloy, homogeneous and functionally graded aluminum (LM25/AlN and LM25/SiO_2) composites. Particul. Sci. Tech. 2019; 37(1):10–20.
[36] Kumar RA, Kumar RK, Radhika N, Mechanical and Wear Properties of Functionally Graded Cu-11Ni-4Si/ Graphite Composite. Silicon 2019; 11:2613–2624.
[37] Hashim J, Looney L, Hashmi MSJ, Particle distribution in cast metal matrix composites—Part I. J. Mater. Proc. Tech. 2002; 123(2):251–257.
[38] Prabhu TR, Processing and study of the wear and friction behaviour of discrete graded Cu hybrid composites. Bull. Mater. Sci. 2015; 38:753–760.
[39] Radhika N, Comparison of the mechanical and wear behavior of aluminum alloy with homogeneous and functionally graded silicon nitride composites. Sci. Eng. Compo. Mater. 2018; 25:261–271.
[40] Vieira AC, Sequeira PD, Gomes JR, Rocha LA, Dry sliding wear of Al alloy/SiC_p functionally graded composites: Influence of processing conditions. Wear; 267(1-4):585–592.
[41] Gomes JR, Miranda AS, Rocha LA, Silva RF, Effect of Functionally Graded Properties on the Tribological Behavior of Aluminum-Matrix Composites. Key Eng. Mat. 2002; 230:271–274.
[42] Radhika N, Jefferson JA, Studies on Mechanical and Abrasive Wear Properties of Cu-Ni-Si/Si_3N_4 Functionally Graded Composite. Silicon 2019; 11:627–641.
[43] Prabhu TR, Processing and properties evaluation of functionally continuous graded 7075 Al alloy/SiC composites. Arch. Civ. Mech. Eng. 2017; 17:20–31.
[44] Radhika N, Raghu R, Experimental investigation on abrasive wear behavior of functionally graded aluminum composite. J. Tribol. 2015; 137:031606.
[45] Radhika N, Raghu R, Effect of Centrifugal Speed in Abrasive Wear Behavior of Al-Si5Cu3/SiC Functionally Graded Composite Fabricated by Centrifugal Casting. Trans. Indian. Inst. Met. 2018; 71:715–726.
[46] Mahli MK, Jamian S, Nor NHM, Nor MKM, Kamarudin KAJ, Effect of Rotating Mold Speed on Microstructure of Al LM6 Hollow Cylinder Fabricated Using Centrifugal Method Phy. Conf. Series 2017; 914:012039.
[47] Rajan TP, Pillai RM, Pai BC, Centrifugal casting of functionally graded aluminum matrix composite components. Int. J. Cast. Met. Res. 2008; 21(1-4): 214–218.
[48] Radhika N, Mechanical Properties and Abrasive Wear Behavior of Functionally Graded Al-Si12Cu/Al_2O_3 Metal Matrix Composite. Trans. Indian. Inst. Met. 2017; 70:145–157.
[49] Radhika N, Raghu R, Study on three-body abrasive wear behavior of functionally graded Al/TiB_2 composite using response surface methodology. Particular, Sci. Tech. 2018; 36(7):816–823.
[50] Jayakumar E, Jacob JC, Rajan TP, Joseph MA, Pai BC, Processing and Characterization of Hypoeutectic Functionally Graded Aluminum – SiC Metal Matrix Composites. Mater. Sci. Forum 2015; 830:456–459.
[51] Radhika N, Thirumalini S, Shivashankar A, Investigation on Mechanical and Adhesive Wear Behavior of Centrifugally Cast Functionally Graded Copper/SiC Metal Matrix Composite. Trans. Indian. Inst. Met. 2018; 71:1311–1322.
[52] Jayakumar E, Praveen AP, Rajan TPD, Pai BC, Studies on Tribological Characteristics of Centrifugally Cast SiCp-Reinforced Functionally Graded A319 Aluminum Matrix Composites. Trans. Indian. Inst. Met. 2018; 71:2741–2748.
[53] Torabinejad V, Aliofkhazraei M, Rouhaghdam AS, Allahyarzadeh M, Tribological performance of Ni-Fe-Al_2O_3 multilayer coatings deposited by pulse electrodeposition. Wear 2017; 380:115-125.

[54] Radhika N, Raghu R, Evaluation of Dry Sliding Wear Characteristics of LM 13 Al/B4C Composites. Tribol. Ind. 2015; 37(1):20–28.
[55] Radhika N, Raghu R, Characterization of mechanical properties and three-body abrasive wear of functionally graded aluminum LM25/titanium carbide metal matrix composite. Materwiss. Werksttech. 2017; 48(9):882–892.
[56] Su B, Yan HG, Chen JH, Zeng PL, Chen G, Chen CC, Wear and Friction Behavior of the Spray-Deposited SiCp/Al-20Si-3Cu Functionally Graded Material. J. Mater. Eng. Perform. 2013; 22:1355–1364.
[57] Prabhu TR, Varma VK, Vedantam S, Tribological and mechanical behavior of multilayer Cu/SiC + Gr hybrid composites for brake friction material applications. Wear 2014; 317(1-2):201–212.
[58] Radhika N, Praveen M, Mukherjee SJ, Influence of process parameters on three body abrasive wear behavior of functionally graded aluminum alloy reinforced with alumina. Eng. Sci. Tech. 2017; 12(11):2866–2879.
[59] Jojith R, Radhika N, Braz J, Fabrication of LM 25/WC functionally graded composite for automotive applications and investigation of its mechanical and wear properties. Soc. Mech. Sci. Eng. 2018; 40:292–301.
[60] Ram SC, Chattopadhyay K, Chakrabarty I, Effect of magnesium content on the microstructure and dry sliding wear behavior of centrifugally cast functionally graded A356-Mg_2Si in situ composites. Mater. Res. Expr. 2018; 5(4):046535.
[61] Arsha AG, Jayakumar E, Rajan TP, Antony V, Pai BC, Design and fabrication of functionally graded in-situ aluminum composites for automotive pistons. Mater. Des. 2015; 88:1201–1209.
[62] Jojith R, Radhika N, Vipin U, Sliding Wear Studies on Heat-Treated Functionally Graded Cu–Ni–Si/TiC Composite. Trans. Indian. Inst. Met. 2019; 72:719–731.
[63] Aravind C, Gopalakrishnan S, Radhika N, Investigating the Adhesive Wear Properties of Aluminum Hybrid Metal Matrix Composites at Elevated Temperatures using RSM Technique. Tribol. Ind. 2019; 41:604–612.
[64] Radhika N, Raghu R, Mechanical and tribological properties of functionally graded aluminum/zirconia metal matrix composite synthesized by centrifugal casting. Int. J. Mater. Res. 2015; 106(11):1174–1181.
[65] Radhika N, Raghu RJ, Synthesis of functionally graded aluminum composite and investigation on its abrasion wear behavior. Eng. Sci. Technol. 2017; 12(5):1386–1398.
[66] Farayibi PK, Folkes JA, Clare AT, Laser Deposition of Ti-6Al-4V Wire with WC Powder for Functionally Graded Components. Mat. Manu. Proce. 2013; 28(5):514–518.
[67] Savas Ö, Ind. Fabrication and characterization of TiB_2-reinforced functionally graded aluminum matrix material. Lubr. Tribol. 2020; 72(10):1147–1152.
[68] Saiyathibrahim A, Subramanian R, Samuel CS, Processing and properties evaluation of centrifugally cast in-situ functionally graded composites reinforced with Al_3Ni and Si particles. Mater. Res. Expre. 2019; 6:1165a8.
[69] Yousefi M, Doostmohammadi H, Spatial and microstructural dependence of mechanical properties and wear performance of functionally graded Al–$TiAl_3$ in situ composite. SN Appl. Sci. 2019; 1:1190–1202.
[70] Ramesh MR, Aithal K, Evaluation of Mechanical and Tribological Properties of Directionally Solidified Al-Si Based FG Composite. Silicon 2020; 12:701–713.
[71] León-Patiño CA, Aguilar-Reyes EA, Bedolla-Becerril E, Bedolla-Jacuinde A, Méndez-Díaz S, Dry sliding wear of gradient Al-Ni/SiC composites. Wear 2013; 301(1-2):688–694.
[72] Ma, G Yu C, Tang B, Li Y, Niu F, Wu D, Bi G, Liu S, High-mass-proportion TiCp/Ti-6Al-4V titanium matrix composites prepared by directed energy deposition. Addit. Manu. 2020; 24:101323.
[73] Kwok JK, Lim SC, High-speed tribological properties of some Al/SiC_p composites: I. Frictional and wear-rate characteristics. Compos. Sci. Tech. 1999; 59(1):55–63.
[74] Haider K, Alam MA, Redhewal A, Saxena V, Investigation of Mechanical Properties of Aluminum Based Metal Matrix Composites Reinforced With Sic & Al_2O_3. Int. J. Eng. Res. Appl. 2015; 5(9):63–69.
[75] Mondal DP, Das S, High stress abrasive wear behaviour of aluminium hard particle composites: Effect of experimental parameters, particle size and volume fraction. Tribol. Int. 2006; 39(6):470–478.
[76] Chinnusamy S, Ramasamy V, Venkatajalapathy S, Kaliyannan GV, Palaniappan SKJ, Experimental investigation on the effect of ceramic coating on the wear resistance of Al6061 substrate. Mater. Res. Tech. 2019; 8(6):6125–6133.
[77] Skopp A, Kelling N, Woydt M, Berger LM, thermally sprayed titanium suboxide coatings for piston ring/cylinder liners under mixed lubrication and dry-running conditions. Wear 2007; 262(9-10):1061–1070.
[78] Zhang QC, Chen X, Han Z, Subsurface morphological pattern, microstructure and wear response of Cu and Cu–Al alloys subjected to unidirectional and reciprocating sliding. Wear 2020; 462:203521.
[79] Rajeev VR, Dwivedi DK, Jain SC, Effect of load and reciprocating velocity on the transition from mild to severe wear behavior of Al–Si–SiC_p composites in reciprocating conditions. Mater. Des. 2010; 31(10):4951–4959.

[80] Lifang X, Zhaohui Y, Jiaxuan L, Effects of intermediate layers on the tribological behavior of DLC coated 2024 aluminum alloy. Wear 2004; 257(5-6):599–605.
[81] Radhika N, Sasikumar J, Sylesh JL, Kishore RJ, Dry reciprocating wear and frictional behavior of B_4C reinforced functionally graded and homogenous aluminum matrix composites. Mater. Res. Tech. 2020; 9(2):1578–1592.
[82] Velhinho A, Botas JD, Avila EA, Gomes JR, Rocha LA, Tribocorrosion Studies in Centrifugally Cast Al-Matrix SiCp-reinforced Functionally Graded Composites. Mater. Sci. Forum 2004; 455:871–875.
[83] Radhika N, Sasikumar J, Arulmozhivarman J, Tribo-Mechanical Behavior of Ti-Based Particulate Reinforced As-Cast and Heat Treated A359 Composites. Silicon 2020; 12:2769–2782.
[84] Rajeev VR, Dwivedi DK, Jain SC, Dry reciprocating wear of Al–Si–SiC_p composites: A statistical analysis. Tribol. Int. 2010; 43(8):1532–1541.
[85] Itoh T, Fujii SJ, Effects of Frequency and Stroke on Lubricated Reciprocating Friction between Plain Carbon Steel and Bearing Steel. Soc. Mater. Sci. 2007; 56(3):266–271.
[86] Harish TV, Rajeev VR, Effect of Variation in Stroke Length on Dry Reciprocating Wear of Aluminum Alloys. Mater. Today 2018; 5(1):1341–1347.
[87] Polajnar M, Kalin M, Thorbjornsson I, Thorgrimsson JT, Valle N, BotorProbierz A, Friction and wear performance of functionally graded ductile iron for brake pads. Wear 2017; 382:85–94.
[88] Harish TV, Rajeev VR, Reciprocating Wear of a A390 Aluminum Alloy Under Varying Stroke Length: A Statistical Analysis to Deduce the Factor Contribution. Int. J. Eng. Adv. Technol. 2019; 8(5):808–814.
[89] Sinha A, Islam MA, Farhat Z, Reciprocating Wear Behavior of Al Alloys: Effect of Porosity and Normal Load. Int. J. Metall. Mater. Eng. 2015; 1:117.
[90] Plint AG, Friction Force Measurement in Reciprocating Tribometers. STLE; 2011.
[91] Lakshmipathy J, Kulendran B, Reciprocating wear behavior of 7075Al/SiC in comparison with 6061Al/Al_2O_3 composites. Int. J. Refract. Hard. Met. 2014; 46:137–144.
[92] Gomes JR, Ramalho A, Gaspar MC, Carvalho SF, Reciprocating wear tests of Al–Si/SiC_p composites: A study of the effect of stroke length. Wear 2005; 259(1-6):545–552.
[93] Jayakumar E, Varghese T, Rajan TP, Pai BC, Reciprocating Wear Analysis of Magnesium-Modified Hyper-eutectic Functionally Graded Aluminum Composites. Trans. Indian. Inst. Met. 2019; 72:1643–1649.
[94] Jojith R, Radhika N, Investigation of Mechanical and Tribological Behavior of Heat-Treated Functionally Graded Al-7Si/B_4C Composite. Silicon 2020; 12:2073–2085.
[95] Cassar G, Wilson JAB, Banfield S, Housden J, Matthews A, Leyland A, A study of the reciprocating-sliding wear performance of plasma surface treated titanium alloy. Wear 2010; 269(1-2):60–70.
[96] Yakovlev A, Bertrand P, Smurov I, Laser cladding of wear resistant metal matrix composite coatings. Thin Solid Films 2004; 453:133–138.
[97] Ortiz M, Penalva M, Iriondo E, López de Lacalle LN, Accuracy and Surface Quality Improvements in the Manufacturing of Ti-6Al-4V Parts Using Hot Single Point Incremental Forming. Metals 2019; 9(6):697–710.
[98] Stachowiak GW, Podsiadlo P, Characterization and classification of wear particles and surfaces. Wear 2001; 249(3-4):194–200.